



Synthesis of (Sty-co-BA-AA) latexes including ZnO and TiO₂ nanoparticle by miniemulsion polymerization

Ali Delibaş

Received: 1 May 2020 / Revised: 12 October 2020 / Accepted: 14 October 2020
© American Coatings Association 2021

Abstract Herein, it is reported that synthesis of poly(styrene-co-butyl acrylate) latexes containing ZnO and TiO₂ nanoparticles was carried out using miniemulsion polymerization. The synthesized latexes and films cast from them were characterized by dynamic light scattering (DLS), X-ray diffraction (XRD), scanning electron microscopy energy dispersive X-ray (SEM-EDAX), transmission electron microscopy (TEM), and thermogravimetric analysis (TGA). Stress-strain and DMA analysis was performed for the mechanical analysis of the films prepared from latexes. The particle sizes of the latexes were about 60 nm for pure latex and latex only containing ZnO and TiO₂, while the particle size for latex containing nanoparticle mixture was measured as 120 nm. XRD, SEM-EDAX, and TEM analysis results showed that the nanoparticles were well dispersed in latex. When the mechanical analysis results were compared, latex films including 2% ZnO nanoparticles were found to be stronger. DMA analysis showed that the glass transition temperature (T_g) values of the polymers were between 0 and 10°C and the nanoparticles were not effective in changing the T_g values. Latex films were exposed to 254 nm UV light to determine their yellowing. According to the colorimetric measurement, ZnO nanoparticle-embedded films were found to be more resistant to yellowing.

Keywords ZnO and TiO₂ nanoparticle, Miniemulsion polymerization, Styrene-co-butyl acrylate-acrylic acid

Introduction

Emulsion polymerization, which includes techniques such as conventional emulsion polymerization, inverse emulsion polymerization, dispersion polymerization, microemulsion polymerization, miniemulsion, and suspension polymerization, is a preferred process in the production of many commonly used polymer applications such as binders, paints, plastics, adhesives, and so on.^{1–3}

Although waterborne latexes, styrene acrylates, are widely preferred in various fields due to their transparency, chemical resistance, weather resistance, mechanical stability, adhesion, and film-forming properties, they do not have good ultraviolet (UV) protection properties for outdoor applications. To prevent UV deterioration, UV absorbers (benzotriazole, benzophenone, etc.), radical scavengers, radical quenchers, and UV protective agents (nano-cerium dioxide, nano-zinc oxide, and nano-titanium dioxide) are preferred as stabilizers.^{4–9} Many chemical approaches such as solution exfoliation, melt intercalation, and in situ polymerization (batch, solution, and heterogeneous polymerization techniques) are used for the preparation of nanocomposites. In recent years, waterborne polymeric nanocomposites prepared by emulsion, miniemulsion, or suspension polymerizations have attracted great attention in academia and industry due to being environmentally friendly and other advantages (cheap, clean, low viscosity, etc.).^{10–12}

Studies on the synthesis of new nanocomposite polymers that greatly improved the properties of the pure polymer with the contributions of the nano-inorganic filler are of great interest for both academia and industry. Inorganic nano fillers such as nanoclay^{12–21}, nano-ZnO^{9,11,22–25}, nano-TiO₂^{4,26–30}, nano-CeO₂^{5,31–35}, nano-iron oxide^{36–38} are mostly used either in pure form or in modified form. Due to the agglomeration and difficulties in the dispersion of nanoparticles in solvent medium and also melting incorporation,

A. Delibaş (✉)
Department of Chemistry, Faculty of Arts and Sciences,
Yozgat Bozok University, 66900 Yozgat, Turkey
e-mail: ali.delibas@bozok.edu.tr

nanocomposite preparation has attracted a great deal of interest in the literature, especially since a Toyota research team reported the exfoliated Nylon 6/clay nanocomposite.³⁹ For example, Erdem and co-workers prepared styrene/encapsulated titania nanoparticles with miniemulsion polymerization using cyclohexane²⁶ and hexadecane²⁷ co-stabilizers. Man et al.⁴ synthesized and characterized rutile TiO₂/poly(methyl methacrylate(MMA)-butyl acrylate(BA)-acrylic acid(AA) nanocomposites via seeded emulsion polymerization and studied their UV-shielding property. González et al.³⁰ synthesized poly(MMA/BA) copolymer-stabilized titania nanoparticles by miniemulsion polymerization and reported that increased TiO₂ content decreased hybrid particle size and film roughness. Moreover, ZnO nanoparticles were incorporated into the MMA, BA, and perfluorooctyl acrylate (FOA) latexes by batch miniemulsion polymerization, and corrosion behavior was investigated by Chimenti et al.⁹ Danková et al.²⁴ synthesized acrylate latex binders by semicontinuous emulsion polymerization using 1.5 wt% ZnO nanoparticles with respect to the polymer content. Chou and coworkers²⁵ synthesized PMMA-b-PBA block copolymer latexes including zinc oxide/poly(sodium 4-styrenesulfonate). Recently, Eren and Can⁴⁰ synthesized the zinc methacrylate-methylmethacrylate-butyl acrylate emulsions by semibatch emulsion polymerization and applied them to exterior paints and reported on the solubility of the ZnO nanoparticles in the medium of methacrylic acid monomer. Also, some authors preferred the combination of ZnO/TiO₂ nanoparticles to achieve more efficient photocatalytic nanoparticles and they used ZnO/TiO₂ nanoparticles combination for photocatalytic removal of a herbicide (Bentazon).⁴¹ Zhang et al.²⁸ successfully synthesized nano ZnO/TiO₂ coupled oxide photocatalyst by a two-step method and applied it for the degradation of methyl orange dye. Magnetic titanium dioxide/polystyrene/magnetite composite hybrid polymer particles were synthesized by Pickering miniemulsion polymerization in one single step and used for degrading methylene blue (MB) from solutions by Bonnefond et al.³⁶

Unlike the above-mentioned literature, for the first time, in this study, it was reported that poly(Sty-co-BA-AA)/ZnO/TiO₂/ZnO-TiO₂ nanocomposite latexes were synthesized by miniemulsion polymerization in one-pot adding (batch-wise). Moreover, incorporation of nanoparticles into the polymer matrix without premodification was accomplished. Synthesized nanocomposite latexes and their films were characterized, and yellowing of the films was assessed.

Experimental

Materials

Styrene (Sty-, purchased from Poliya Company, Turkey), butyl acrylate (BA-supplied kindly from

KEMPRO Company, Turkey) and acrylic acid (AA-purchased from ZAG Kimya, Turkey) monomers were used in the study after distillation in darkness under reduced pressure to remove the inhibitors and stored in a refrigerator before use. Ammonium persulfate (APS), sodium bicarbonate (SBC), and sodium dodecyl sulfate (SDS) were used as the initiator, to adjust the pH and emulsifier, respectively, and they were obtained from Merck. The hexadecane (HD) used in the study was purchased from Sigma-Aldrich and used as is. ZnO nanoparticle with 40-100 nm particle size and 10–25 m²/g surface area was supplied from Alfa Aesar. The rutile TiO₂ nanoparticles with < 100 nm particle size and trace metal basis used in the study were Aldrich brand. Deionized water (Mes, MP Minipure, Turkey) was used as solvent throughout the study.

Experimental procedure

Synthesis studies of nanoparticle-added latexes containing various proportions of ZnO and TiO₂ were carried out with a total ~ 30% solids. All studies were achieved using 50/50% styrene/butyl acrylate monomer ratios and 2 g of acrylic acid (neutralized completely with NaOH solution). To ensure that the ZnO and TiO₂ nanoparticles remain stable in latex, the general method for the synthesis of latexes was applied as follows.

The emulsifier, nanoparticles (ZnO, TiO₂, and ZnO/TiO₂), monomers, hexadecane, and deionized water were weighed in appropriate amounts according to the total solid content (see Table 1) and were mixed overnight. The temperature was kept low to avoid polymerization. Then, the mixture was first subjected to ultrasonic treatment in the ultrasonic bath (Kudos, 53 kHz frequency) for 20 min, and then, it was mixed with the homogenizer (IKA T18 digital ULTRA TURRAX) at 8000 rpm to obtain pre-emulsion. The

Table 1: Miniemulsion polymerization recipe for nanocomposite latexes

Component	Amount (g)	Pphm
<i>Oil Phase</i>		
Sty	19.5	50.0
BA	19.5	50.0
HD	1.56	4.00
ZnO-TiO ₂	0.20-0.78	0.5-2.0
<i>Aqueous phase</i>		
SDS	1.56	4.00
Deionized water	91.0	233.3
AA*	3.25	8.30
SBC	0.16	0.40
APS	0.30	0.77

Pphm: parts per hundred monomer; solid content ≈30%; * AA completely neutralized with NaOH solution (50%)

pre-emulsified colloidal mixture was transferred to the polymerization reactor, the temperature of which was adjusted to 75 °C, to fulfill the polymerization. All the experiments were carried out in batch-wise (one-pot synthesis). The system was stirred at 260 rpm with the help of a mechanical stirrer (Heidolph). After the system reached the desired temperature, the reaction was started by adding initiator (APS). Five hours later, the reaction was terminated by cooling the reactor. After the filtration of the latex with the glass frit of pore size 1 to separate the coagulum, samples were stored in closed containers to prevent evaporation in the dark, protected from sunlight.

To prepare latex films, 20 mL of synthesized latex was taken and poured into petri dishes and allowed to dry in the dark. Dried latex films were taken from petri dishes and kept for UV tests and mechanical analysis in a way that they do not receive light.

Characterization

The solids content (SC) of the latexes was measured with Radwag MA 110R model infrared heater moisture analyzer. After separating the coagulum from the reaction product, the solid content of the latexes was determined taking into account the amount of auxiliary materials. Zeta potential values and the z average particle size (D_i -nm) were measured with Zetasizer Nano ZS, Malvern Instruments. XRD diffraction analysis was performed with PANalytical—Empyrean using Cu K α radiation ($\lambda = 0.15406$ nm, 40 mA, 45 kV, Step Size ° [2Th.] 0.0260). TGA analysis was performed at 10°C/min heating rate in 25–600°C temperature range with PerkinElmer Diamond instrument in nitrogen atmosphere. Electron diffraction analyses were performed by suspension preparation on carbon-coated copper grids and imaged with transmission electron microscope (TEM) using Jeol JSM 3010 300 kV, and TEM micrographs were obtained with JEOL JEM 1220. EDAX analyses of the latex films were examined by field emission–environmental scanning electron microscope–energy distribution spectrometry (FE-ESEM-EDS) (FEIQuanta 450 FEG) to obtain surface images and characterize the elemental composition. Stress–strain analysis was carried out with SHIMADZU AG-XD 50kN device with 5 mm/min shrinkage speed, and results were given as the average of three measurements. DMA analysis was carried out with SHIMADZU AG-XD 50kN device with 5 mm/min shrinkage speed and with PerkinElmer DMA 8000 device, with 3°C/min heating speed, 1 Hz vibration frequency, 0.05 mm/min shrinkage speed, and between – 60 and 100°C range, respectively. To examine the changes of latex films under UV light, the latex films were exposed to UV light of 254 nm for 96 h in the UV cabinet. Color measurements of samples were performed with Data-color 400 brand color measurement instrument.

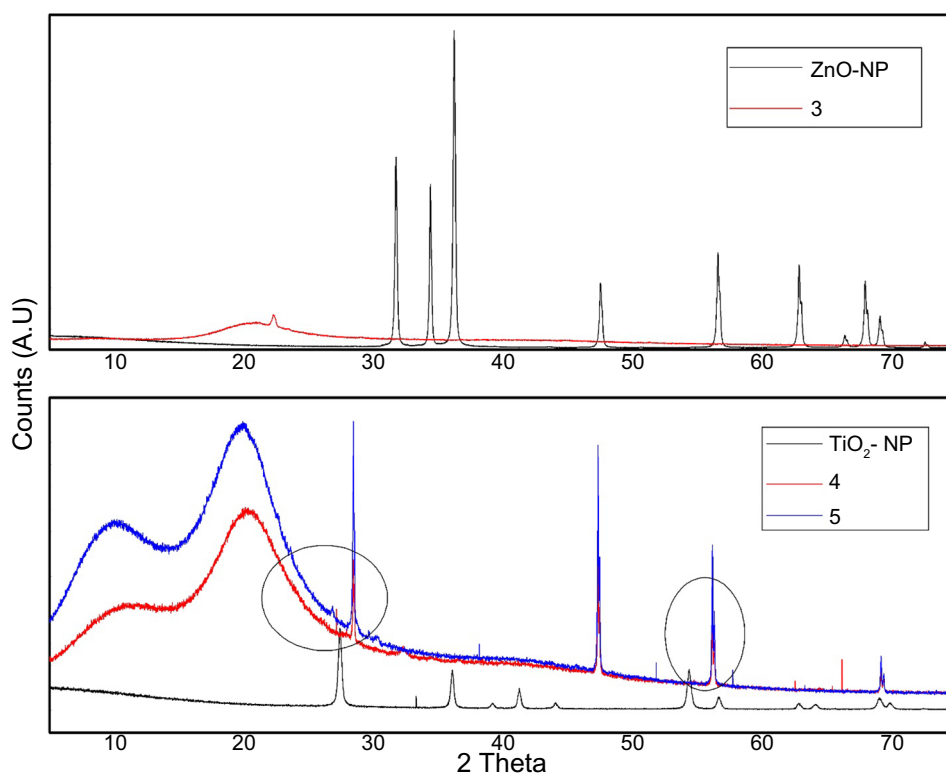
Results and discussion

When nanoparticle-filled latexes are obtained, it is expected that no coagulation occurs, the particles do not precipitate over time, and the resulting latex remains stable during the waiting period (such as no phase separation, solidification, film formation). At this point, miniemulsion polymerization was used as a preferable approach to obtain stable latex droplets. To this end, the effects of different parameters for the synthesis of ZnO and TiO₂ nanoparticle-filled latexes were examined. Stability of the latexes and sedimentation problem of the nanoparticle were observed in the study conducted with different ratios of emulsifier and nanoparticle without acrylic acid (AA) and hexadecane (HD). In addition, since acrylic acid caused dissolution of ZnO nanoparticles and coagulation, neutralized acrylic acid was used in subsequent experiments.⁴¹ In polymerization experiments using acrylic acid and hexadecane, the best results were achieved using 8% AA, 4% HD, and 4% SDS (based on the amount of monomer). Furthermore, SBC and APS amounts were used as 0.5% and 0.75%, respectively, according to the monomer amount. Some properties of latexes with different ratios of ZnO and TiO₂ nanoparticles prepared using these optimum conditions are given in Table 2.

The solids content, zeta potential values, and particle sizes of the synthesized latexes are shown in Table 2. Considering the recipe used in latex synthesis, the theoretically calculated amount of solid content was $\approx 30\%$. Table 2 shows that the results are very close to the theoretical results in all experiments and conversions are close to 100%. Particle sizes are given as a z-mean result. When the particle size analysis results are examined, the particle sizes of the latex containing ZnO and TiO₂ nanoparticles alone are close to sample 1 (pristine polymer latex) and not dependent on the nanoparticle amount. In contrast, in the latexes containing both nanoparticles together (sample 6, 7 and 8), particle sizes were observed to increase up to 120 nm. Although it is known that the particle sizes increase with the addition of nanoparticles,^{10,30,33,42,43} there is no literature regarding the increase in particle size by adding ZnO and TiO₂ nanoparticle together. Faucheu et al.⁴³ reported an increase in particle size with increased amount of clay for clay/MMA-BA composite polymers prepared using water soluble initiator and miniemulsion polymerization. Similar cases were also reported by Leiza and co-workers. Interestingly, Romo-Urbe et al.⁴⁴ reported that the latex (MMA/BA/AA) particle size remained about constant (140 nm) with nano-SiO₂ concentrations. As shown in Table 2, zeta potential values indicate that stable latexes were obtained; especially, ZnO/TiO₂ nanoparticle mixtures seem to be more effective on the stability of latexes.

Table 2: Effect of nanoparticles on SC, zeta potential, and particle size

Sample No.	TiO ₂ (%)	ZnO (%)	SC%	Zeta Potential (mV)	(D _r) (nm)
1	–	–	29.3	– 68.2	59
2	–	1	30.8	– 48.6	61
3	–	2	29.3	– 71.6	60
4	1	–	29.6	– 59.0	54
5	2	–	30.0	– 61.8	51
6	0.5	1	30.1	– 83.8	118
7	1	1	31.3	– 88.5	120
8	0.5	0.5	30.5	– 84.7	123

**Fig. 1: XRD patterns of the ZnO-TiO₂ nanoparticles and latex films of sample 3 (2% ZnO), sample 4 (1% TiO₂) and sample 5 (2% TiO₂)**

XRD results

XRD patterns of TiO₂ and ZnO nanoparticles and latex films containing these nanoparticles are given in Fig. 1. As shown in Fig. 1, latex films containing TiO₂ had diffraction peaks originating from TiO₂, and the intensity of these peaks appropriately increased with TiO₂ concentration. No diffraction peak was observed for the latexes including ZnO nanoparticle. This could be explained by the fact that ZnO nanoparticles randomly dispersed in latex and exfoliated nanocomposite formation.^{13,17} However, it was also reported by Youssef, et al, while diffraction peak was observed in

high ZnO loadings, no diffraction peak was observed in low ZnO loadings.⁴⁵ Additionally, diffraction peaks in the TiO₂ containing film were sharper and shifted relative to the diffraction peaks of the TiO₂ nanoparticles themselves which could be evaluated as an indication of aggregation of the TiO₂.

TGA results

TGA analysis of filmed latex samples was performed to examine whether there was a change in the thermal stability of latex samples. TGA curves are given in

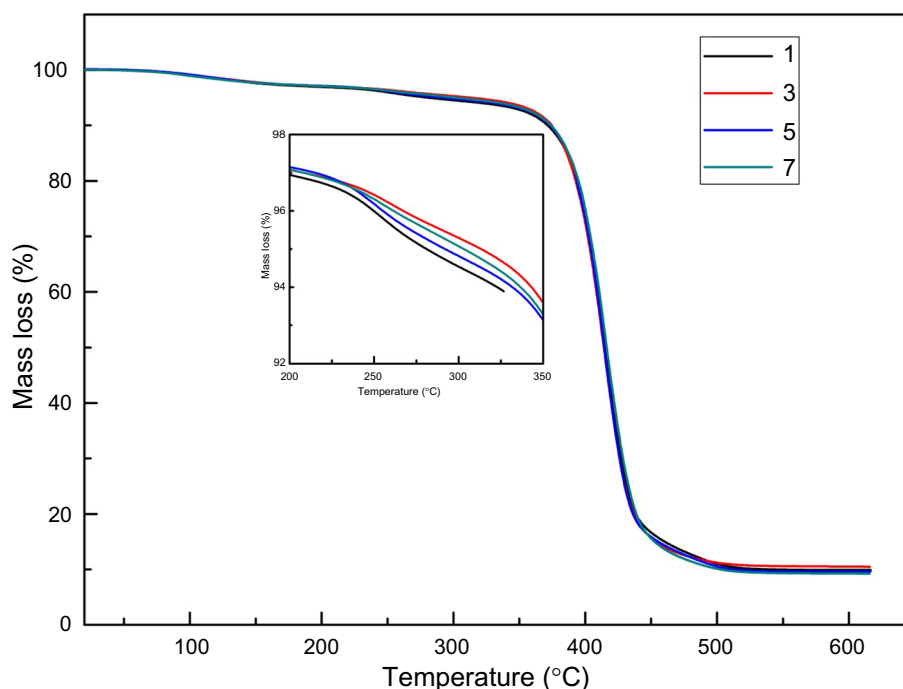


Fig. 2: Thermograms of the latex film and nanocomposite latex films

Fig. 2. As shown in Fig. 2, latex and nanoparticle-added latex films were thought to exhibit two-stage degradation and the first degradation step was between 80 and 150°C and about 3% mass loss, which were due to water loss. When the detailed graph given in Fig. 2 for the second degradation step (225°C initial) was investigated, it was observed that the latex without nanoparticle was more easily degraded, and the ZnO nanoparticles increased thermal stability more than TiO₂. This increased thermal stability could be attributed to crosslinking agent behavior of the ZnO nanoparticles.^{6,46} Likewise, it has been stated in the literature that ZnO nanoparticles are capable of self-crosslinking in latex containing neutralized carboxylic groups in the wet state and during drying at room temperature.^{47,48} Since sample 5 contains both ZnO and TiO₂ nanoparticles, its thermal stability remained between the ZnO including latex film and TiO₂ including latex film. When the residue amounts were compared, it was noted that latex films containing ZnO showed the highest thermal resistance.

SEM and TEM results

SEM images and EDAX analysis results of latex films containing ZnO and TiO₂ nanoparticles are given in Fig. 3 with $\times 50k$ magnification. As seen from EDAX results in Fig. 3, it is clear that ZnO and TiO₂ nanoparticles were incorporated into the latex. In addition, it was seen from the SEM images that the nanoparticles were distributed within the latex, with some being homogeneous in some places, and others

demonstrating agglomeration in some places. The reason could be attributed to the aggregation of nanoparticles during film formation from the latex. However, as seen from the SEM images (Fig. 3c) of the latex containing nanoparticle mixture, it was seen that the nanoparticle distribution was more homogeneous; in other words, there was no agglomeration. This could be interpreted as a positive synergistic effect on nanoparticle distribution when nanoparticles were used together. When the TEM images, given in Fig. 4 are examined, it is clearly seen that the nanoparticle sizes vary in the range of 30–70 nm and the particles are dispersed in the latex even though there is agglomeration. It is also noteworthy that in Figs. 4a and 4b, the ZnO nanoparticles are encapsulated.⁴² Moreover, the dark lines between the polymer particles show the pinhole effect reported by Tauer et al.^{10,49} Additionally, images of the electron diffraction analysis in the TEM (selected area electron diffraction-SAED) are given for sample 3 (2% ZnO) and sample 5 (2% TiO₂) (see Figs. 4e and 4f). Considering the copolymer composition (component that can make diffraction), diffraction rings with different images evidently demonstrate that latex samples contain ZnO and TiO₂ nanoparticles.

Mechanical properties of the latex films

Stress-strain analysis and DMA (dynamic mechanical analysis) were performed as three parallel studies to determine the mechanical properties of the films obtained from the synthesized latex. When Table 3

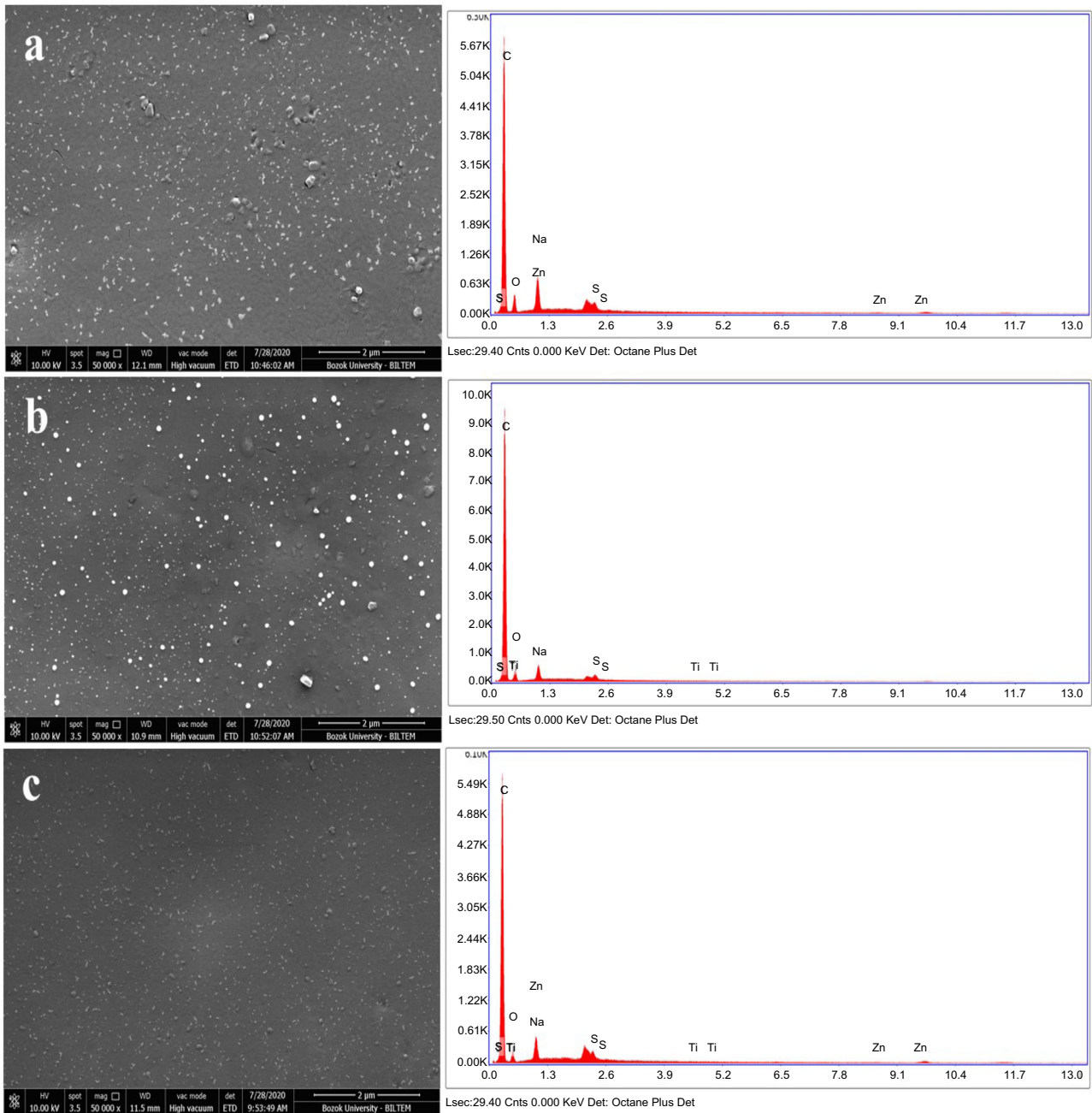


Fig. 3: SEM images and EDAX analyses (a) film of sample 3 (2% ZnO) (b) film of sample 5 (2% TiO₂) (c) of sample 7 (mixture of 1% ZnO-1% TiO₂)

and Fig. 5 are examined together, it is understood that ZnO-embedded latex films had the highest mechanical strength due to crosslinking effect mentioned in thermal properties section, and considering samples 6, 7, and 8, ZnO was more effective than TiO₂ in view of increasing the mechanical properties of latex films. Table 3 shows that the maximum force was already observed in sample 3 containing 2% ZnO nanoparticle. Although it was understood that the results of the pristine latex film (sample 1) showed good resistance compared to the nanocomposite films, the film thick-

ness should not be neglected. In particular, the mechanical strength of latexes containing 1% ZnO and 1% TiO₂ nanoparticle samples seems to be quite good considering the film thicknesses. The modulus vs temperature curves of the obtained latex films are given in Fig. 6a. As shown in Fig. 6a, there was a slight decrease in the modulus values of the latex films incorporated into the nanoparticle, and this decrease was not as much in both the glassy state and the rubbery region for the films containing 2% ZnO. This decrease appeared to be greater in films alone con-

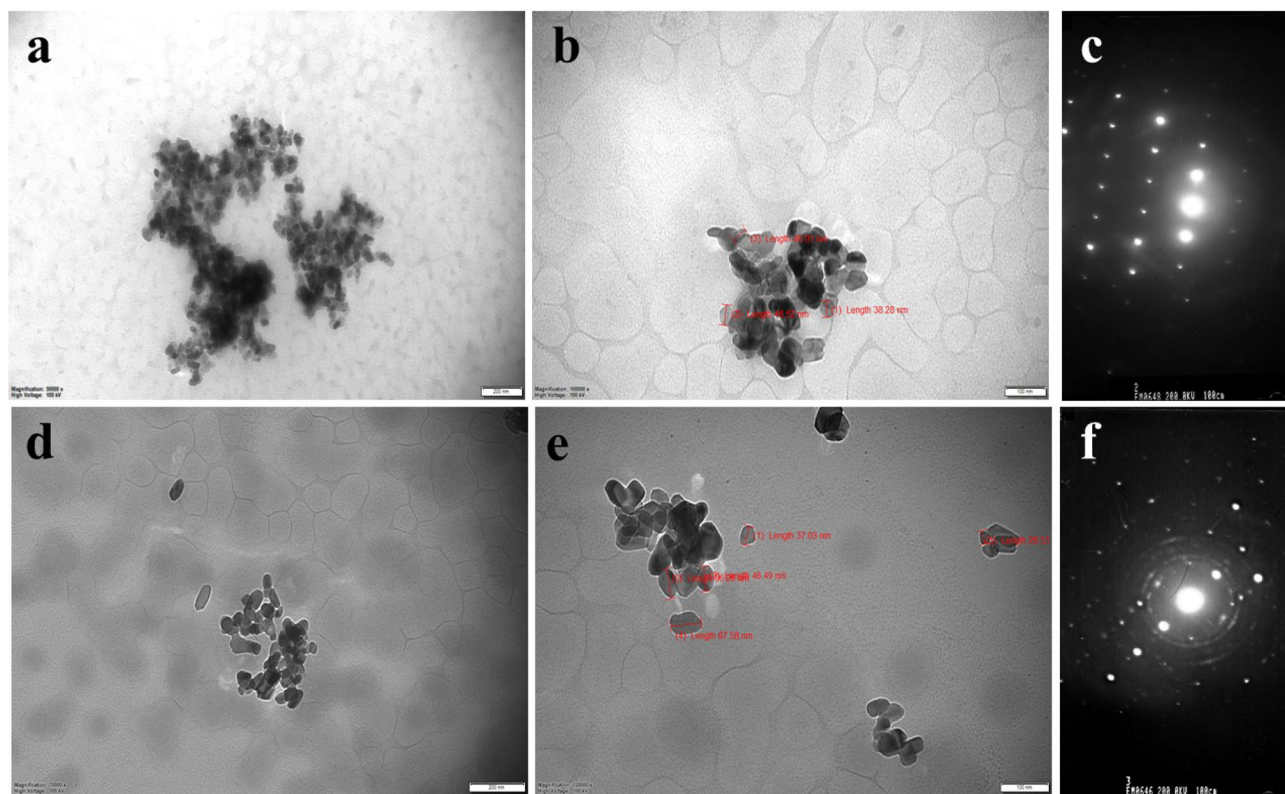


Fig. 4: TEM micrographs of sample 3 with 2% ZnO (a) scale 200 nm (b) scale 100 nm (c) electron diffraction and sample 5 with 2% TiO₂ (d) scale 200 nm (e) scale 100 nm (f) electron diffraction

Table 3: Stress–strain results of the prepared latex films

Sample No.	Max. force all area (N)	Max. stress all area (N/mm ²)	Max. strain (%)	Sample thickness (mm)
1	27.8 ± 8.1	3.74 ± 0.36	814 ± 242	0.96 ± 0.07
2	31.1 ± 4.2	2.63 ± 0.77	771 ± 214	1.09 ± 0.18
3	32.3 ± 6.2	4.44 ± 0.39	929 ± 197	0.87 ± 0.06
4	21.4 ± 5.5	2.86 ± 0.21	542 ± 226	0.80 ± 0.17
5	21.3 ± 3.0	3.46 ± 0.70	683 ± 122	0.84 ± 0.10
6	25.2 ± 7.9	2.97 ± 0.29	665 ± 174	0.69 ± 0.16
7	26.5 ± 7.9	4.26 ± 0.43	865 ± 128	0.69 ± 0.11
8	14.3 ± 6.2	3.69 ± 1.49	491 ± 144	0.75 ± 0.17

taining TiO₂ and the mixture (1% ZnO and 1% TiO₂). While the mechanical properties of latex films containing nanoparticles were expected to increase, this loss in modulus was thought to be related to decrease in molecular weight with the addition of nanoparticles.^{13,50} The curves of Tan δ vs temperature of latex films are given in Fig. 6. As shown in Fig. 6, the temperature at which polymer films began to soften, i.e., T_g values, was almost the same. The \sim T_g value calculated from the Fox equation for the Sty-BA-AA (sodium acrylate in this study) copolymer composition in this study is around + 15°C. As shown in Fig. 5.7, in the synthesized latex films, a transition from glassy to rubbery was observed below this temperature (0–

10°C). Nanoparticles appeared to slightly widen the curve. This can be interpreted as a decrease in glass transition temperature, especially for samples 5 and 7. This can be explained by the fact that the incorporated nanoparticles supplied plasticizing properties to the latex films, even to a small extent.⁵⁰

Yellowing test of the latex films

Color measurement results of latex films kept under UV light for 96 h are presented in Table 4. Given delta b values in Table 4 were measured based on measuring

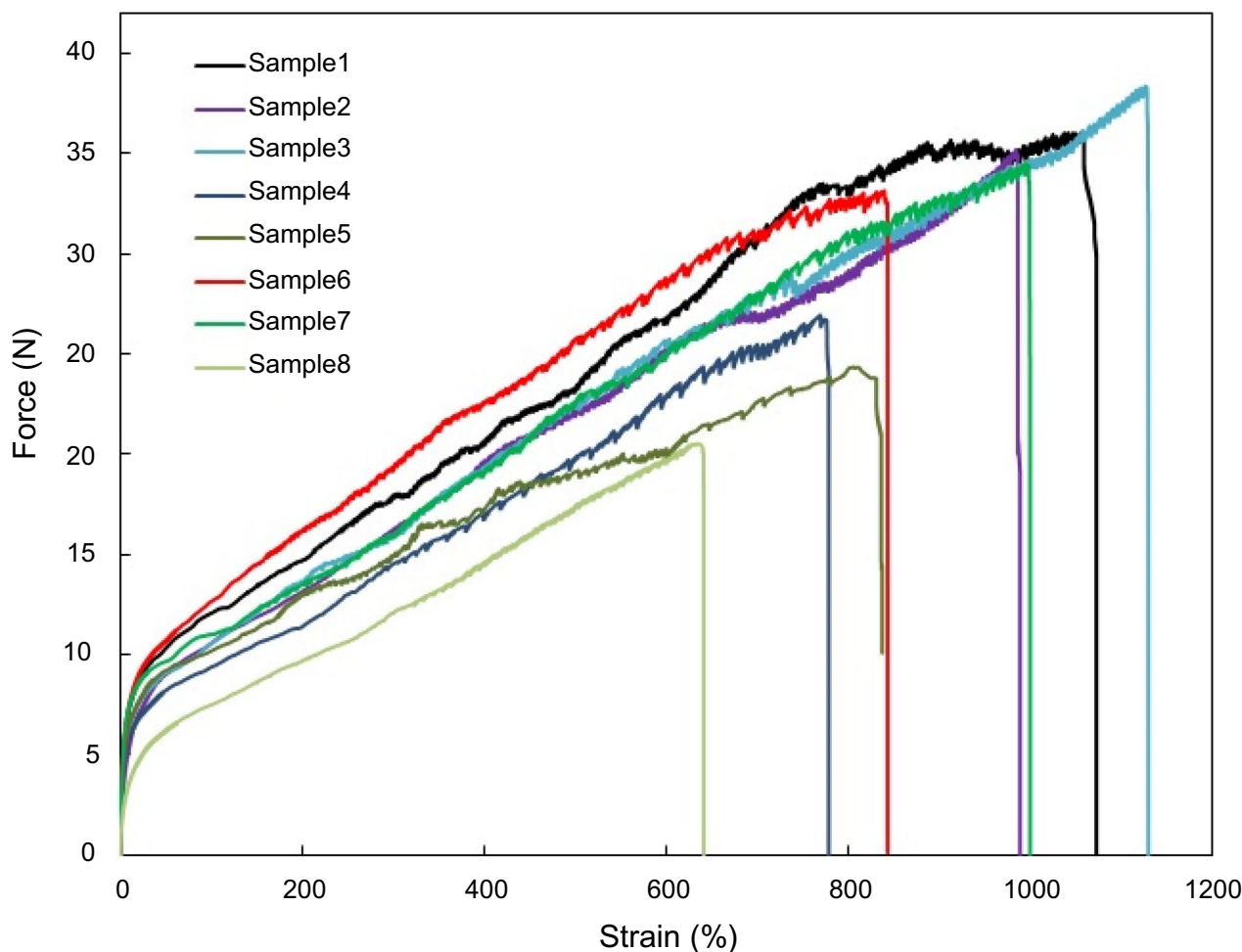


Fig. 5: Stress–strain curves of the prepared latex films

the difference in color between exposed and masked portions of the same film. The value of $-b$ means that the samples move away without yellowing, and $+b$ values mean that the samples turn yellow.^{30,51} When Table 4 is examined according to this definition, yellowing occurred in sample 1, which is pristine latex film. Except for sample 4, it is seen that the latex film samples with nanoparticle are effective against yellowing and move away from yellowing. It is concluded that the most effective condition against yellowing was in sample 6; less than 2% TiO_2 and less than 1% ZnO nanoparticles were not effective against yellowing and ZnO was more effective than TiO_2 against yellowing.

Conclusions

The composite latexes containing the ZnO and TiO_2 nanoparticles were investigated to meet the conditions (emulsifier amount, HD amount, AA amount), such as the formation of coagulum, the nanoparticles not

collapsing over time, and the stability of the obtained latex during the waiting period. As a result of the work done:

- AA should be used in a neutralized way
- Stable latexes cannot be obtained when using HD less than 4%
- It is concluded that 4% SDS amount is sufficient for obtaining 30% solid latex, and latexes synthesized under these conditions are stable from the zeta potential data

Results obtained from SEM-EDAX and TEM analysis show that nanoparticles were dispersed in latex. It is concluded that nanoparticles partially increase the thermal stability of latex films. From the stress–strain analysis results of the latex films, especially ZnO nanoparticles caused an increase in strength due to ZnO crosslinking effect. It is understood from the DMA analysis results that the films began to change from glassy to rubber in the range of 0–10°C,

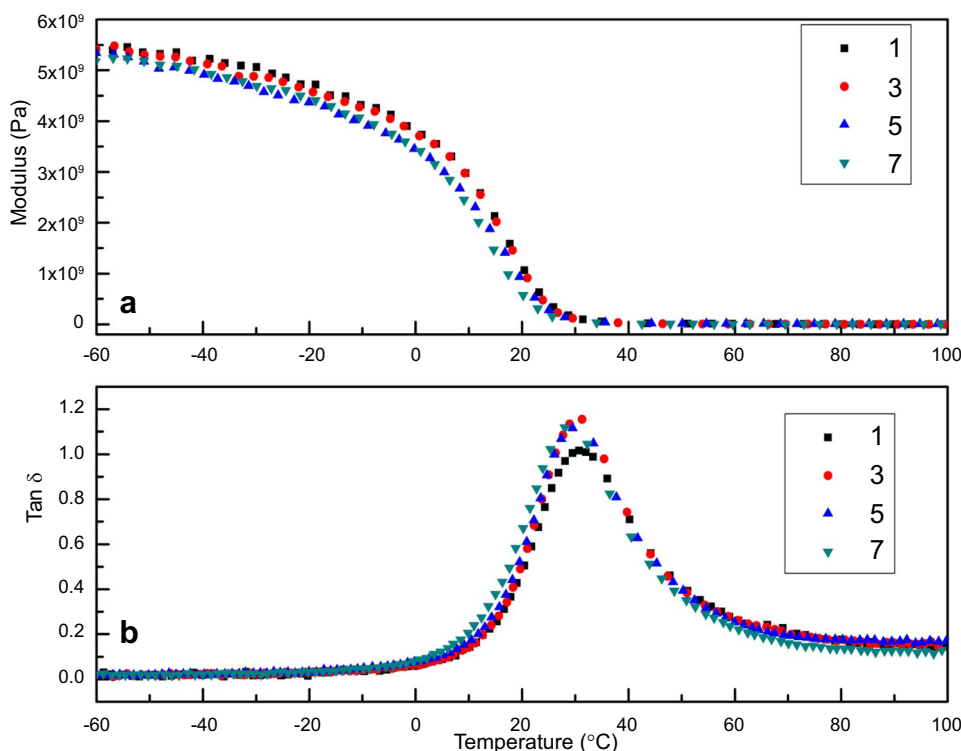


Fig. 6: Curves obtained by DMA analysis (a) modulus vs temperature (b) Tan δ vs temperature

Table 4: Yellowing results of the latex films

Sample No.	TiO ₂ (%)	ZnO (%)	Δb
1	–	–	2.53
2	–	1	– 3.58
3	–	2	– 4.12
4	1	–	2.83
5	2	–	– 0.80
6	0.5	1	– 8.33
7	1	1	– 3.66
8	0.5	0.5	– 1.46

and nanoparticles did not change this value much. As a result of the yellowing test, ZnO- and TiO₂-doped latex films showed better resistance to yellowing caused by UV light and ZnO was more effective for yellowing than TiO₂.

Acknowledgments Thanks to Scientific Research Projects Unit of Yozgat Bozok University (Grant no. 6602c-FEF/16-12) for the financial support. Thanks to Dr. Ramazan Coşkun for his valuable comments.

Conflict of interest The authors declare that they have no conflict of interest.

References

1. Erbil, Y, *Vinyl Acetate Emulsion Polymerization and Copolymerization with Acrylic Monomers*. CRC Press, Boca Raton (2000)
2. Lovell, PA, El-Aasser, MS, *Emulsion Polymerization and Emulsion Polymers*. Wiley, Hoboken (1997)
3. Dieter, U, Takamura, K, *Polymer Dispersions and Their Industrial Applications*. Wiley VCH Verlag GmbH & Co, KGaA (2002)
4. Man, YK, Mu, LY, Wang, Y, Lin, SH, Rempel, GL, Pan, QM, “Synthesis and Characterization of Rutile Titanium Dioxide/Polyacrylate Nanocomposites for Applications in Ultraviolet Light-Shielding Materials.” *Polym. Comp.*, **36** (1) 8–16 (2015)
5. Aquirre, M, Paulis, M Leiza, JR, “Waterborne Acrylic/CeO₂ Nanocomposites for UV Blocking Clear Coats,” In: Khan, S, Akhtor, K (Eds) *Cerium Oxide—Applications and Attributes*, Intechopen (2018)
6. Tang, EJ, Liu, H, Sun, LM, Zheng, EL, Cheng, GX, “Fabrication of Zinc Oxide/poly(styrene) Grafted Nanocomposite Latex and its Dispersion.” *Europ. Polym. J.*, **43** (10) 4210–4218 (2007)
7. Hu, J, Chen, M, Wu, LM, “Organic-inorganic Nanocomposites Synthesized via Miniemulsion Polymerization.” *Polym. Chem.*, **2** (4) 760–772 (2011)
8. Hu, J, Zhou, Y, “The Properties of Nano(ZnO-CeO₂)@polysiloxane Core-shell Microspheres and Their Application for Fabricating Optical Diffusers.” *Appl. Surf. Sci.*, **365** 166–170 (2016)
9. Chimentì, S, Vega, JM, Aguirre, M, García-Lecina, E, Díez, JA, Grande, H-J, Paulis, M, Leiza, JR, “Effective Incorporation of ZnO Nanoparticles by Miniemulsion Polymeriza-

- tion in Waterborne Binders for Steel Corrosion Protection.” *J. Coat. Technol. Res.*, **14** (4) 829–839 (2017)
10. Delibas, A, Yildiz, U, Tauer, K, “Composite Latex Production with High Solid Content.” *J. Appl. Polym. Sci.*, **136** 18 (2019)
 11. Tang, EJ, Dong, SY, “Preparation of Styrene Polymer/ZnO Nanocomposite Latex via Miniemulsion Polymerization and its Antibacterial Property.” *Colloid Polym. Sci.*, **287** (9) 1025–1032 (2009)
 12. Diaconu, G, Paulis, M, Leiza, JR, “High Solids Content Waterborne Acrylic/Montmorillonite Nanocomposites by Miniemulsion Polymerization.” *Macromol. React. Eng.*, **2** (1) 80–89 (2008)
 13. Zengeni, E, Hartmann, PC, Pasch, H, “Highly Filled Polystyrene/Laponite Hybrid Nanoparticles Prepared Using the Ad-Miniemulsion Polymerisation Technique.” *Macromol. Chem. Phys.*, **214** (1) 62–75 (2013)
 14. Bonnefond, A, Paulis, M, Bon, SAF, Leiza, JR, “Surfactant-free Miniemulsion Polymerization of n-BA/S Stabilized by NaMMT: Films with Improved Water Resistance.” *Langmuir*, **29** (7) 2397–2405 (2013)
 15. Herrera, NN, Letoffe, JM, Putaux, JL, David, L, Bourgeat-Lami, E, “Aqueous Dispersions of Silane-functionalized Laponite Clay Platelets. A First Step toward the Elaboration of Water-based Polymer/Clay Nanocomposites.” *Langmuir*, **20** (5) 1564–1571 (2004)
 16. Kang, BA, Schrade, A, Xu, Y, Chan, YT, Ziener, U, “Synthesis and Characterization of Dually Labeled Pickering-type Stabilized Polymer Nanoparticles in a Downscaled Miniemulsion System.” *Langmuir*, **28** (25) 9347–9354 (2012)
 17. Yilmaz, O, Cheaburu, CN, Gülümser, G, Vasile, C, “On the Stability and Properties of the Polyacrylate/Na-MMT Nanocomposite Obtained by Seeded Emulsion Polymerization.” *Europ. Polym. J.*, **48** (10) 1683–1695 (2012)
 18. Ruggerone, R, Plummer, CJG, Herrera, NN, Bourgeat-Lami, E, Månson, J-AE, “Highly Filled Polystyrene-laponite Nanocomposites Prepared by Emulsion Polymerization.” *Europ. Polym. J.*, **45** (3) 621–629 (2009)
 19. Plummer, CJG, Ruggerone, R, Bourgeat-Lami, E, Manson, JAE, “Small Strain Mechanical Properties of Latex-based Acrylic Nanocomposite Films.” *Polym.*, **52** (9) 2009–2015 (2011)
 20. Diaconu, G, Micusik, M, Bonnefond, A, Paulis, M, Leiza, JR, “Macroinitiator and Macromonomer Modified Montmorillonite for the Synthesis of Acrylic/MMT Nanocomposite Latexes.” *Macromol.*, **42** (9) 3316–3325 (2009)
 21. Sheibat-Othman, N, Cenacchi-Pereira, AM, Dos Santos, AM, Bourgeat-Lami, E, “A Kinetic Investigation of Surfactant-free Emulsion polymerization of Styrene Using Laponite Clay Platelets as Stabilizers.” *J. Polym. Sci. Part A: Polym. Chem.*, **49** (22) 4771–4784 (2011)
 22. Christopher, G, Anbu Kulandainathan, M, Harichandran, G, “Highly Dispersive Waterborne Polyurethane/ZnO Nanocomposites for Corrosion Protection.” *J. Coat. Technol. Res.*, **12** (4) 657–667 (2015)
 23. Gu, X, Chen, G, Zhao, M, Watson, SS, Nguyen, T, Chin, JW, Martin, JW, “Critical Role of Particle/Polymer Interface in Photostability of Nano-filled Polymeric Coatings.” *J. Coat. Technol. Res.*, **9** (3) 251–267 (2012)
 24. Danková, M, Kalendová, A, Machotová, J, “Waterborne Coatings based on Acrylic Latex Containing Nanostructured ZnO as an Active Additive.” *J. Coat. Technol. Res.*, **17** (2) 517–529 (2020)
 25. Chou, IC, Lee, CF, Chiu, WY, “Preparation of Novel Suspensions of ZnO/Living Block Copolymer Latex Nanoparticles via Pickering Emulsion Polymerization and Their Long Term Stability.” *J. Polym. Sci. Part A: Polym. Chem.*, **49** (16) 3524–3535 (2011)
 26. Erdem, B, Sudol, ED, Dimonie, VL, El-Aasser, MS, “Encapsulation of Inorganic Particles via Miniemulsion polymerization. I. Dispersion of Titanium Dioxide Particles in Organic Media Using OLOA 370 as Stabilizer.” *J. Polym. Sci. Part A: Polym. Chem.*, **38** (24) 4419–4430 (2000)
 27. Erdem, B, Sudol, ED, Dimonie, VL, El-Aasser, MS, “Encapsulation of Inorganic Particles via Miniemulsion Polymerization. II. Preparation and Characterization of Styrene Miniemulsion Doplets Containing TiO₂ Particles.” *J. Polym. Sci. Part A: Polym. Chem.*, **38** (24) 4431–4440 (2000)
 28. Zhang, M, Gao, G, Li, C-Q, Liu, F-Q, “Titania-Coated Polystyrene Hybrid Microballs Prepared with Miniemulsion Polymerization.” *Langmuir*, **20** (4) 1420–1424 (2004)
 29. Wu, YF, Zhang, Y, Xu, JX, Chen, M, Wu, LM, “One-Step Preparation of PS/TiO₂ Nanocomposite Particles via Miniemulsion Polymerization.” *J. Colloid Interf. Sci.*, **343** (1) 18–24 (2010)
 30. Gonzalez, E, Bonnefond, A, Barrado, M, Barrasa, AMC, Asua, JM, Leiza, JR, “Photoactive Self-cleaning Polymer Coatings by TiO₂ Nanoparticle Pickering Miniemulsion Polymerization.” *Chem. Eng. J.*, **281** 209–217 (2015)
 31. Ma, Q, Izu, N, Masuda, Y, “Ceria Polymer Hybrid Nanoparticles and Assembled Films for Coating Applications.” *ACS Appl. Nano Mater.*, **1** (5) 2112–2119 (2018)
 32. Incel, A, Güner, T, Parlak, O, Demir, MM, “Null Extinction of Ceria@Silica Hybrid Particles: Transparent Polystyrene Composites.” *ACS Appl. Mater. Interfaces*, **7** (49) 27539–27546 (2015)
 33. Aguirre, M, Paulis, M, Leiza, JR, “Particle Nucleation and Growth in Seeded Semibatch Miniemulsion Polymerization of Hybrid CeO₂/Acrylic Latexes.” *Polym.*, **55** (3) 752–761 (2014)
 34. Zgheib, N, Putaux, J-L, Thill, A, D’Agosto, F, Lansalot, M, Bourgeat-Lami, E, “Stabilization of Miniemulsion Droplets by Cerium Oxide Nanoparticles: a Step Toward the Elaboration of Armored Composite Latexes.” *Langmuir*, **28** (14) 6163–6174 (2012)
 35. Garnier, J, Warnant, J, Lacroix-Desmazes, P, Dufils, P-E, Vinas, J, van Herk, A, “Sulfonated Macro-RAFT Agents for the Surfactant-free Synthesis of Cerium Oxide-based Hybrid Latexes.” *J. Colloid Interf. Sci.*, **407** 273–281 (2013)
 36. Bonnefond, A, Ibarra, M, Gonzalez, E, Barrado, M, Chuvilin, A, Maria Asua, J, Ramon Leiza, J, “Photocatalytic and Magnetic Titanium Dioxide/Polystyrene/Magnetite Composite Hybrid Polymer Particles.” *J. Polym. Sci. Part A: Polym. Chem.*, **54** (20) 3350–3356 (2016)
 37. Mori, Y, Kawaguchi, H, “Impact of Initiators in Preparing Magnetic Polymer Particles by Miniemulsion Polymerization.” *Colloids Surf. B: Biointerfaces*, **56** (1) 246–254 (2007)
 38. Staudt, T, Machado, TO, Vogel, N, Weiss, CK, Araujo, PHH, Sayer, C, Landfester, K, “Magnetic Polymer/Nickel Hybrid Nanoparticles via Miniemulsion Polymerization.” *Macromol. Chem. Phys.*, **214** (19) 2213–2222 (2013)
 39. Kojima, Y, Usuki, A, Kawasumi, M, Okada, A, Fukushima, Y, Kurauchi, T, Kamigaito, O, “Mechanical Properties of Nylon 6-clay Hybrid.” *J. Mater. Res.*, **8** (5) 1185–1189 (1993)
 40. Eren, M, Can, HK, “Preparation of Zinc Methacrylate-methylmethacrylate-butyl Acrylate Emulsions and Their Application in Exterior Paints.” *Prog. Org. Coat.*, **135** 424–437 (2019)
 41. Gholami, M, Shirzad-Siboni, M, Farzadkia, M, Yang, J-K, “Synthesis, Characterization, and Application of ZnO/TiO₂ Nanocomposite for Photocatalysis of a Herbicide (Bentazon).” *Desalin. Water Treat.*, **57** (29) 13632–13644 (2016)

42. Aguirre, M, Barrado, M, Iturrondobeitia, M, Okariz, A, Guraya, T, Paulis, M, Leiza, JR, “Film Forming Hybrid Acrylic/ZnO Latexes with Excellent UV Absorption Capacity.” *Chem. Eng. J.*, **270** 300–308 (2015)
43. Faucheu, J, Gauthier, C, Chazeau, L, Cavaille, JY, Mellon, V, Bourgeat-Lami, E, “Miniemulsion Polymerization for Synthesis of Structured Clay/Polymer Nanocomposites: Short Review and Recent Advances.” *Polym.*, **51** (1) 6–17 (2010)
44. Romo-Uribe, A, Arcos-Casarrubias, JA, Hernandez-Vargas, ML, Reyes-Mayer, A, Aguilar-Franco, M, Bagdhachi, J, “Acrylate Hybrid Nanocomposite Coatings Based on SiO₂ Nanoparticles by In-situ Batch Emulsion Polymerization.” *Prog. Org. Coat.*, **97** 288–300 (2016)
45. Youssef, A, El-Nagar, I, El-Torky, A and El-Hakim, AEFA, “Preparation and Characterization of PMMA Nanocomposites Based on ZnO-NPs for Antibacterial Packaging Applications.” *Proc. World Congress on New Technologies*, (2019)
46. Sonawane, SH, Teo, BM, Brotchie, A, Grieser, F, Ashokkumar, M, “Sonochemical Synthesis of ZnO Encapsulated Functional Nanolatex and Its Anticorrosive Performance.” *Ind. & Eng. Chem. Res.*, **49** (5) 2200–2205 (2010)
47. Lee, DI, “The Effects of Latex Coalescence and Interfacial Crosslinking on the Mechanical Properties of Latex Films.” *Polym.*, **46** (4) 1287–1293 (2005)
48. Pinprayoon, O, Saiani, A, Groves, R, Saunders, BR, “Particulate Ionomer Films Prepared from Dispersions of Cross-linked Polymer Colloids: a Structure–Property Study.” *J. Colloid Interf. Sci.*, **336** (1) 73–81 (2009)
49. Schellenberg, C, Tauer, K, Antonietti, M, “Film Formation of Polymeric Emulsions: Structure Set-up and the Pinhole Effect Characterized by Microscopic Techniques.” *J. Dispersion Sci. Technol.*, **20** (1–2) 177–186 (1999)
50. Samakande, A, Sanderson, RD, Hartmann, PC, “Encapsulated Clay Particles in Polystyrene by RAFT Mediated Miniemulsion Polymerization.” *J. Polym. Sci. Part A: Polym. Chem.*, **46** (21) 7114–7126 (2008)
51. Ruot, B, Plassais, A, Olive, F, Guillot, L, Bonafous, L, “TiO₂-Containing Cement Pastes and Mortars: Measurements of the Photocatalytic Efficiency Using a Rhodamine B-based Colourimetric Test.” *Solar Energy*, **83** (10) 1794–1801 (2009)

Publisher’s Note Springer Nature remains neutral with regard to jurisdictional claims in published maps and institutional affiliations.